

DSC STUDY OF GLYCEROL-EXTRACTED MUSCLE FIBERS IN INTERMEDIATE STATES OF ATP HYDROLYSIS

T. Dergez¹, F. Könczöl², N. Farkas¹, J. Belágyi¹ and D. Lőrinczy^{3*}

¹Institute of Bioanalysis, Faculty of Medicine, University of Pécs, Szigeti str. 12, 7624 Pécs, Hungary

²Institute of Forensic Medicine, Faculty of Medicine, University of Pécs, Szigeti str. 12, 7624 Pécs, Hungary

³Institute of Biophysics, Faculty of Medicine, University of Pécs, Szigeti str. 12, 7624 Pécs, Hungary

The heat capacity of contractile proteins actin and myosin was studied in psoas muscle of rabbit in strongly and weakly binding state of myosin to actin as a function of temperature by DSC. Deconvolution of the unfolding scans makes possible to characterize the structural domains of the macromolecules. We tried to approach the unfolding process in different intermediate state of ATP hydrolysis. The thermal transitions were calorimetrically irreversible, therefore the two-state irreversible model that describes fairly well the denaturation of different proteins was used for evaluation of the denaturation processes in muscle fibers in strongly (rigor, ADP) and weakly binding states (ATP·V_i, ADP·AlF₄) of myosin to actin. Deconvolution resulted in four transitions, the first three transition temperatures were almost independent of the intermediate states of muscle, the last transition temperature was shifted to higher temperature, when the buffer solution was manipulated. The mean values in strongly binding states were $T_{m1}=52.9\pm 0.7$ °C, $T_{m2}=57.9\pm 0.7$ °C, $T_{m3}=63.7\pm 1.0$ °C and $T_{m4}=67.8\pm 0.7$ °C, but the last transition increased to higher temperature depending on the P_i analogue.

Keywords: ATP hydrolysis, deconvolution of DSC scans, DSC, muscle fiber

Introduction

The muscle contraction and other events of cell motility are based on [1–8] the cyclic interaction of the head portion of myosin with actin during the myosin-catalyzed ATP hydrolysis. It is also known from earlier studies that AM**·ADP·P_i complex (A denotes actin and M stands for myosin and P_i is inorganic phosphate) is the predominant intermediate of the ATP hydrolysis cycle in the actomyosin system. In isolated form of myosin the half-life is only several seconds at 25°C, therefore further stabilization is needed in muscle fibres to perform detailed structural or dynamic analysis of this transition state. It was found that a complex of myosin with ADP and orthovanadate formed a stable structure, which allowed the studies on the conformation in this intermediate [9, 10]. The crystal structure of *Dictyostelium* myosin looks similar to chicken myosin without nucleotides, while other complexes exhibited large changes in the head of myosin [11].

In the present study we examined by differential scanning calorimeter (DSC) the main intermediate steps of ATP hydrolysis cycle (complexes of myosin with ADP and ADP+V_i (where V_i is orthovanadate, an inorganic phosphate analogue)) in muscle fibres to see the relationship between global structural changes in the actomyosin complex. DSC measurements on the modified actomyosin complexes revealed significant conformational changes, the thermal stability of the

nucleotide-binding domain markedly increased in ADP+V_i state. To find the possible structural domains that could undergo some rearrangement we have applied Fourier deconvolution of DSC signals based on the recent thermodynamic model of the treatment of irreversibly denatured macromolecular systems [12–16].

Experimental

Materials

Potassium chloride (KCl), magnesium chloride (MgCl₂), ethylene glycol-*bis*(β-aminoethyl ether)-N,N'-tetraacetic acid (EGTA), histidine·HCl, glycerol, adenosine 5'-diphosphate (ADP), adenosine 5'-triphosphate (ATP), and orthovanadate, phosphoenol pyruvic acid, pyruvate kinase, lactic dehydrogenase were obtained from Sigma (Germany).

Fiber preparation

Glycerol-extracted muscle fiber bundles were prepared from rabbit psoas muscle. Small stripes of muscle fibers were stored after osmotic shocks in 50% v/v glycerol and rigor solution (100 mM KCl, 5 mM MgCl₂, 1 mM EGTA, 10 mM histidine·HCl, pH 7.0) at –18°C up to one month. In DSC experiments the fiber bundles of glycerinated muscle were

* Author for correspondence: denes.lorinczy@aok.pte.hu

washed for 60 min in rigor buffer to remove glycerol, and then transferred to fresh buffer and homogenized. This state models the rigor state of the muscle. MgADP was added of 5 mM concentration to the rigor solution to simulate the strongly binding state of myosin that may correspond to the AM·ADP state. The other analogues of intermediates in the ATPase pathway were formed by ATP (5 mM) and orthovanadate (5 mM, abbreviated V_i) which together bind stoichiometrically at the active site of myosin to form a stable complex, $AM^+ \cdot ADP \cdot X_i$ (where M^+ represents a myosin isomer and X_i stands for a nucleotide). This complex is believed to be analogue of the steady-state intermediate $AM^{**} \cdot ADP \cdot P_i$.

Calorimetric measurements

The thermal unfolding of muscle fibers in different states were monitored by a Setaram Micro DSC-II calorimeter. All experiments were done between 0 and 100°C. 0.3 K min⁻¹ was used as a scan rate. Conventional Hastelloy batch vessels were used during the denaturation experiments with 850 µL sample volume in average. Rigor buffer was used as reference sample. The sample and reference vessels were equilibrated with a precision of ±0.1 mg. There was no need to do any correction from the point of view of heat capacity between the sample and reference vessels. The Setaram two-point fitting integration software was used to calculate the calorimetric enthalpy.

ATPase activity

The ATPase activity was determined using a pyruvate kinase–lactate dehydrogenase coupled optical test [17]. The assay medium for Mg²⁺-ATPase consisted of 100 mM KCl, 20 mM MOPS, 1 mM MgCl₂, 0.5 mM EGTA, 0.15 mM NADH, 1 mM phosphoenol pyruvic acid, 20 U mL⁻¹ pyruvate kinase, 40 U mL⁻¹ lactic dehydrogenase, 0.5 mM ATP, pH 7.0. For Ca²⁺-Mg²⁺-ATPase: assay medium plus 1 mM CaCl₂. At 340 nm the absorbance change was measured with a PerkinElmer spectrophotometer interfaced to a computer. The molar absorption coefficient of NADH was ϵ (340 nm)=6.22·10³ mol⁻¹ cm⁻¹. In the experiments the Mg²⁺-ATPase and the Ca²⁺-Mg²⁺-ATPase

activities of thin fiber bundles over 10 min intervals were determined. The decrease of fluorescence resulted in a straight line, the slope of the straight line was used to estimate the ATPase activity. We assumed that 50% of the dried muscle weight was myosin. The Mg²⁺-ATPase activity (µmol of P_i/mg myosin·min) was 4.131±0.718 (*n*=4). The ATPase activity of active fiber bundles was 5.565±0.816 µmol of P_i/mg myosin·min (*n*=4).

Results and discussion

Evaluation of thermal transitions in muscle fibers

The reversibility of denaturation was checked by comparing the first scan of the muscle fibers with the second one after cooling the sample to room temperature. The DSC transitions were calorimetrically irreversible. The first DSC trace was corrected for the calorimetric base line by subtracting the second scan from the first one and for the difference in heat capacity by using a linear base line. In strong and weakly actin binding states the thermograms could be decomposed into three separate transitions in the main transition temperature range (from 40 to 85°C). Considering the muscle structure a fourth heat transition was also assumed which was assigned to actin. Deconvolution into four components was performed by using PeakFit 4.0 software from SPSS Corporation. For analysis of the single thermal transitions Gaussian functions were assumed. The comparison between the DSC patterns in different states of the fiber bundles suggested that the second and third Gaussian curves represented the myosin rod and the actin moiety. The results are included in Table 1. The most striking feature of the traces is that the transition temperature of the last peak strongly depends on the intermediate states of the muscle. Similar observations were obtained on isolated myosin subfragment 1 [18–20]. Figures 1 and 2 show the deconvolution of DSC traces into single components for rigor fibers and fibers in weakly binding state of myosin to actin. This later state was achieved by incubating the fibers in rigor buffer containing ATP and orthovanadate. The incubation lasted for 10 min before DSC measurements.

Table 1 DSC results on muscle fibres: transition temperatures in range of 40–85°C. Glycerinated muscle fibres prepared from psoas muscle of rabbit were measured in rigor, strongly and weakly binding state of myosin to actin. The transition temperatures were derived from the original DSC curves

Experimental results	$T_{m1}/^{\circ}\text{C}$	$T_{m2}/^{\circ}\text{C}$	$T_{m3}/^{\circ}\text{C}$	$T_{m4}/^{\circ}\text{C}$
rigor	52.2	59.2	–	67.8
ADP	53.0	57.8	–	67.8
ATP· V_i	53.6	57.8	63.3	68.9

Mean values: $T_{m1}=52.9\pm0.7^{\circ}\text{C}$ (*n*=9), $T_{m2}=57.9\pm0.7^{\circ}\text{C}$ (*n*=9), $T_{m3}=63.7\pm1.0^{\circ}\text{C}$ (*n*=7)

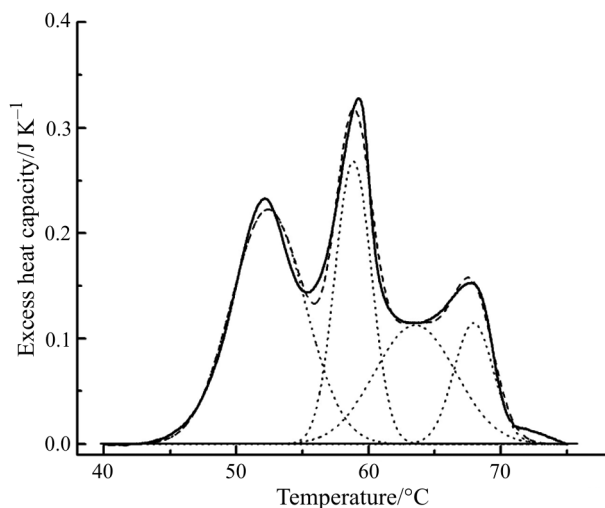


Fig. 1 DSC transition of muscle fibres in rigor. The excess heat capacity curve was deconvoluted using PeakFit 4.0 software of SPSS Corporation. Solid line shows the original DSC trace, whereas dashed line represents the superposition of deconvoluted (dotted) curves

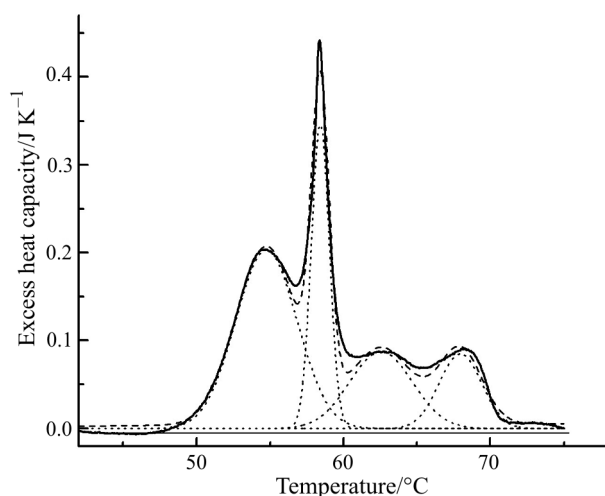


Fig. 2 Excess heat capacity curve of muscle fibres in AM·ADP·V_i state. Deconvolution was performed by PeakFit 4.0 software. Solid line shows the original DSC transitions, dashed line is the result of superposition of single transitions

The simplest model, which can be applied for irreversible transitions, was suggested by Lumry and Eyring [12]. Later on, Sanchez-Ruiz *et al.* reported that the two-state irreversible model describes fairly well the denaturation of different proteins [13, 14, 16]. The theory assumed a reversible unfolding of the proteins that is followed by a rate-limiting irreversible step:



where F means the final state of the irreversible denatured protein. The extent of the irreversibility is determined by the rate constant k_2 of the D→F step, and its activation energy gives the rate of unfolding. Recently, it was shown that in some cases the thermodynamic parameters could be deduced from the standard treatment of the heat capacity curves [15].

According to the results the transition temperatures depend on scan rate, therefore it can be assumed that kinetic processes determined the melting of the muscle samples. The scan rate practically reached its maximum value at about 0.5 K min⁻¹, therefore it permitted to apply a deconvolution of the complex DSC patterns with Gaussian functions (Table 2). The deconvolution resulted in four transitions, the first three transition temperatures were almost independent of the intermediate state of the muscle, the last transition temperature was shifted to higher temperature (~68°C), when the buffer solution was manipulated to mimic the intermediate states of ATP hydrolysis. The mean values were $T_{m1}=52.9\pm 0.7^\circ\text{C}$ ($n=9$), $T_{m2}=57.9\pm 0.7^\circ\text{C}$ ($n=10$), $T_{m3}=63.7\pm 1.0^\circ\text{C}$ ($n=7$).

Thermal transitions in rigor muscle

Earlier measurements performed on myosin showed that at least five endothermic transitions could be observed on bovine heart myosin between the temperature range of 20–55°C [21, 22]. The structure formation of proteins in fibers alters the dynamic and energetic properties of the proteins, the consequence of that is the shift of the melting points 39, 47 and 51°C, measured in solution on intact myosin from rabbit psoas muscle, to higher temperatures in rigor (Fig. 1).

Table 2 Deconvolution of DSC patterns. Deconvolution was performed by using PeakFit 4.0 software from SPSS Corporation. For analysis of the single thermal transitions Gaussian functions were assumed. The transition enthalpies are given in % of the total enthalpy. The transition temperatures and enthalpies were obtained from the deconvoluted curves

Results of deconvolution	$T_1/^\circ\text{C}$	$T_2/^\circ\text{C}$	$T_3/^\circ\text{C}$	$T_4/^\circ\text{C}$
rigor	52.4	58.8	63.5	67.9
area/%	41.2	24.6	22.9	11.4
ADP	53.2	57.6	61.5	67.1
area/%	42.6	21.2	21.9	14.3
ATP·V _i	54.4	57.4	63.1	69.5
area/%	39.5	21.3	21.1	18.1

This is evidence that particular regions of myosin are subjected to stabilizing forces in the filament system leading to alteration of the transition temperatures.

Effect of ATP and orthovanadate on thermal transitions

The comparison of the DSC patterns in strongly and weakly binding states of myosin to actin in fiber bundles showed that the transition temperature at the second and third transitions varied only slightly, whereas the last one (the fourth transition) shifted markedly to higher temperature [23–25]. Treating the fiber bundles in buffer solution containing ATP and V_i , they can produce the weakly binding state (Fig. 2). For direct comparison of the intermediate states the DSC curves were deconvoluted. Assuming Gaussian curves for the thermal transitions of myosin rod and actin filaments in muscle fibers, their transition curves were subsequently subtracted from the original DSC curve (Figs 3 and 4). In order to obtain reasonable residuals the melting temperatures of the transitions, the contributions of the individual Gaussian curves to the total endothermic transition and their line widths at half-height of the transition temperature were varied during the manipulation. The great asymmetry of the first residuals suggests that this transition is very likely the superposition of transitions arising from domains of myosin head. One candidate might be the subfragment 2. In an experiment to interpret the multiple peaks of heavy meromyosin in the DSC scan, it was suggested that the first endotherm peak at 41°C could be due to melting of subfragment 2 [26]. The actin-based order of myo-

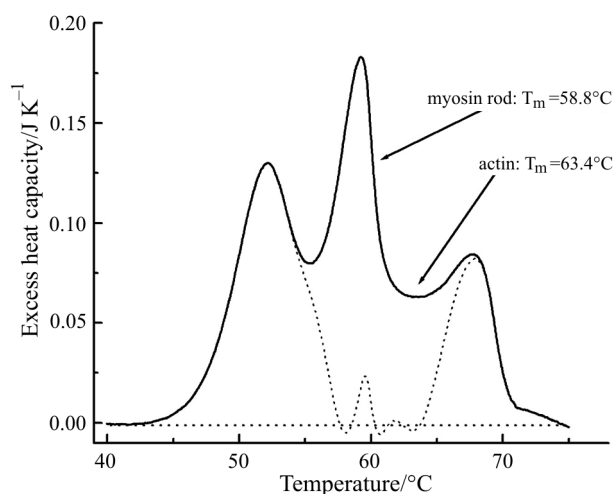


Fig. 3 Excess heat capacity curve of muscle fibres in rigor after manipulation (dotted line). The melting curves of myosin rod and actin filaments were subtracted from the complex DSC transition. The line widths at half-height, the location and the contribution of the single transitions were varied. The values of line widths are $\delta W_{rod}=3.64^\circ\text{C}$ and $\delta W_{actin}=3.99^\circ\text{C}$

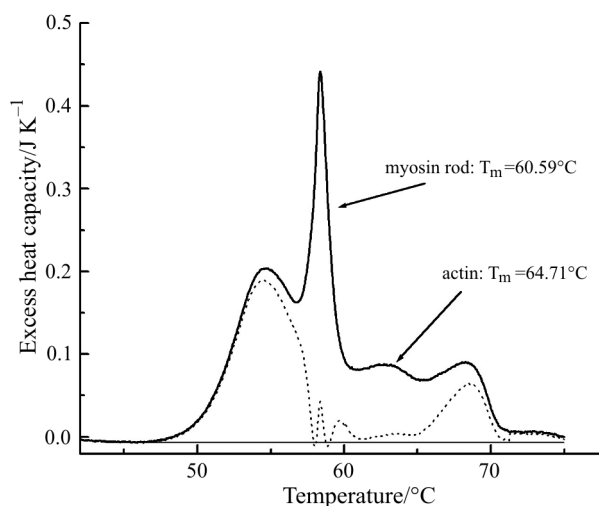


Fig. 4 Excess heat capacity curve of the intermediate state $\text{ADP}\cdot V_i$ after manipulation (dotted line). The melting curves of myosin rod and actin filaments were subtracted from the complex DSC transition. The line widths at half-height, the location and the contribution of the single transitions were varied. The values of line widths are $\delta W_{rod}=1.25^\circ\text{C}$ and $\delta W_{actin}=7.85^\circ\text{C}$

sin heads in rigor changes in weakly binding state and this leads to changes of the line width at half-height. The changes of the internal order of myosin filaments and the flexibility changes of actin filaments in nucleotide-free state and in the presence of nucleotides result in changes of the cooperativity.

The areas are proportional to the transition enthalpy of the protein domains. The sum of the areas under the first and last curves was practically constant, but their fractions depended on the state of the muscle. In strongly binding state of myosin to actin (rigor, ADP state) the fraction of the first transition was much larger, than the last one, whereas in weakly binding state of myosin to actin, the fraction of the first transition decreased at the expense of the last one. It supports also the view that these transitions are parts of the same portion of the myosin molecule.

Conclusions

Using deconvolution procedures on the DSC traces of muscle fiber bundles four single transitions could be derived and assigned to actin binding domain, myosin rod and actin at temperatures of 52.9 ± 0.7 , 57.9 ± 0.7 , $63.7\pm 1.0^\circ\text{C}$. The temperature of the highest transition, which is very likely in connection with the nucleotide-binding domain, depends on the intermediate state of the ATP hydrolysis.

Significant difference was found between the strongly and weakly binding states of myosin to actin.

ADP trapped by V_i on myosin head induced remarkable stabilization in the globular part of myosin, which is reflected in a 2.0–6.0°C shift of the transition temperature to higher temperature. Neglecting the small changes observed in the linewidth of transitions at half-height for myosin rod and actin filaments, we can conclude that the global conformational changes mostly occur in the globular portion of myosin heads in muscle fibers.

Acknowledgements

This work was supported by grant from the National Research Foundation (OTKA T 030248). The SETARAM Micro DSC-II used in the experiments were purchased with funds provided by the National Research Foundation Grant CO-272.

References

- 1 M. A. Geeves, *Biochem. J.*, 274 (1991) 1.
- 2 K. C. Holmes, *Acta Cryst.*, A54 (1998) 789.
- 3 K. C. Holmes, *Nat. Struct. Biol.*, 5 (1998) 940.
- 4 M. A. Geeves and K. C. Holmes, *Annu. Rev. Biochem.*, 68 (1999) 687.
- 5 I. Rayment, H. M. Holden, M. Whittaker, C. B. Yohn, M. Lorenz, K. C. Holmes and R. A. Milligan, *Science*, 261 (1993) 58.
- 6 R. Dominguez, Y. Freyzon, K. M. Trybus and C. Cohen, *Cell*, 94 (1998) 659.
- 7 A. J. Fisher, C. A. Smith, J. Thoden, R. Smith, K. Sutoh, H. M. Holden and I. Rayment, *Biophys. J.*, 68 (1995) 19s.
- 8 A. J. Fisher, C. A. Smith, J. Thoden, R. Smith, K. Sutoh, H. M. Holden and I. Rayment, *Biochemistry*, 34 (1995) 6581.
- 9 C. C. Goodno, *Proc. Natl. Acad. Sci. USA*, 76 (1979) 2620.
- 10 C. Wells and C. R. Bagshaw, *J. Muscle Res. Cell Motil.*, 5 (1984) 97.
- 11 A. M. Gulick, C. B. Bauer, J. B. Thoden and I. Rayment, *Biochemistry*, 36 (1997) 11619.
- 12 R. Lumry and H. Eyring, *J. Phys. Chem.*, 58 (1954) 110.
- 13 J. M. Sanchez-Ruiz, J. L. Lopez-Lacomba, M. Cortijo and P. L. Mateo, *Biochemistry*, 27 (1988) 1648.
- 14 F. Conjero-Lara, P. L. Mateo, F. X. Aviles and J. M. Sanchez-Ruiz, *Biochemistry*, 30 (1991) 2067.
- 15 T. Vogl, C. Jatzke, H.-J. Hinz, J. Benz and R. Huber, *Biochemistry*, 36 (1997) 1657.
- 16 M. Thorolfsson, B. Ibarra-Molero, P. Fojan, S. B. Petersen, J. M. Sanchez-Ruiz and A. Martinez, *Biochemistry*, 41 (2002) 7573.
- 17 D. R. Trentham, R. G. Bardsley, J. P. Eccleston and A. G. Weeds, *Biochem. J.*, 126 (1972) 635.
- 18 D. I. Levitsky, V. L. Shnyrov, N. V. Khvorov, A. F. Bukatina, N. S. Vedenkina, E. A. Permyakov, O. P. Nikolaeva and B. F. Poglazov, *Eur. J. Biochem.*, 209 (1992) 829.
- 19 A. Bobkov, N. K. Khovorov, N. L. Golitsina and D. I. Levitsky, *FEBS Lett.*, 332 (1993) 64.
- 20 D. Lőrinczy and J. Belágyi, *Biophys. Biochem. Res. Commun.*, 217 (1995) 592.
- 21 K. Samejima, M. Ishioroshi and T. Yashui, *Agric. Biol. Chem.*, 47 (1983) 2373.
- 22 A. Bertazzon and T. Y. Tsong, *Biochemistry*, 29 (1990) 6447.
- 23 D. Lőrinczy, F. Könczöl, L. Farkas, J. Belágyi and C. Schick, *J. Therm. Anal. Cal.*, 66 (2001) 633.
- 24 M. Kiss, J. Belágyi and D. Lőrinczy, *J. Therm. Anal. Cal.*, 72 (2003) 565.
- 25 D. Lőrinczy, M. Kiss and J. Belágyi, *J. Therm. Anal. Cal.*, 72 (2003) 573.
- 26 A. Setton and A. Muhrad, *Arch. Biochem. Biophys.*, 235 (1984) 411.